

Improved measurement of time-dependent CP asymmetries and the CP -odd fraction in the decay $B^0 \rightarrow D^{*+} D^{*-}$

B. Aubert,¹ M. Bona,¹ D. Boutigny,¹ Y. Karyotakis,¹ J. P. Lees,¹ V. Poireau,¹ X. Prudent,¹ V. Tisserand,¹ A. Zghiche,¹ J. Garra Tico,² E. Grauges,² L. Lopez,³ A. Palano,³ M. Pappagallo,³ G. Eigen,⁴ B. Stugu,⁴ L. Sun,⁴ G. S. Abrams,⁵ M. Battaglia,⁵ D. N. Brown,⁵ J. Button-Shafer,⁵ R. N. Cahn,⁵ Y. Groyzman,⁵ R. G. Jacobsen,⁵ J. A. Kadyk,⁵ L. T. Kerth,⁵ Yu. G. Kolomoisky,⁵ G. Kukartsev,⁵ D. Lopes Pegna,⁵ G. Lynch,⁵ L. M. Mir,⁵ T. J. Orimoto,⁵ I. L. Osipenkov,⁵ M. T. Ronan,^{5,*} K. Tackmann,⁵ T. Tanabe,⁵ W. A. Wenzel,⁵ P. del Amo Sanchez,⁶ C. M. Hawkes,⁶ A. T. Watson,⁶ H. Koch,⁷ T. Schroeder,⁷ D. Walker,⁸ D. J. Asgeirsson,⁹ T. Cuhadar-Donszelmann,⁹ B. G. Fulsom,⁹ C. Hearty,⁹ T. S. Mattison,⁹ J. A. McKenna,⁹ A. Khan,¹⁰ M. Saleem,¹⁰ L. Teodorescu,¹⁰ V. E. Blinov,¹¹ A. D. Bukin,¹¹ V. P. Druzhinin,¹¹ V. B. Golubev,¹¹ A. P. Onuchin,¹¹ S. I. Serednyakov,¹¹ Yu. I. Skovpen,¹¹ E. P. Solodov,¹¹ K. Yu. Todyshev,¹¹ M. Bondioli,¹² S. Curry,¹² I. Eschrich,¹² D. Kirkby,¹² A. J. Lankford,¹² P. Lund,¹² M. Mandelkern,¹² E. C. Martin,¹² D. P. Stoker,¹² S. Abachi,¹³ C. Buchanan,¹³ S. D. Foulkes,¹⁴ J. W. Gary,¹⁴ F. Liu,¹⁴ O. Long,¹⁴ B. C. Shen,¹⁴ G. M. Vitug,¹⁴ L. Zhang,¹⁴ H. P. Paar,¹⁵ S. Rahatlou,¹⁵ V. Sharma,¹⁵ J. W. Berryhill,¹⁶ C. Campagnari,¹⁶ A. Cunha,¹⁶ B. Dahmes,¹⁶ T. M. Hong,¹⁶ D. Kovalskyi,¹⁶ J. D. Richman,¹⁶ T. W. Beck,¹⁷ A. M. Eisner,¹⁷ C. J. Flacco,¹⁷ C. A. Heusch,¹⁷ J. Kroseberg,¹⁷ W. S. Lockman,¹⁷ T. Schalk,¹⁷ B. A. Schumm,¹⁷ A. Seiden,¹⁷ M. G. Wilson,¹⁷ L. O. Winstrom,¹⁷ E. Chen,¹⁸ C. H. Cheng,¹⁸ F. Fang,¹⁸ D. G. Hitlin,¹⁸ I. Narsky,¹⁸ T. Piatenko,¹⁸ F. C. Porter,¹⁸ R. Andreassen,¹⁹ G. Mancinelli,¹⁹ B. T. Meadows,¹⁹ K. Mishra,¹⁹ M. D. Sokoloff,¹⁹ F. Blanc,²⁰ P. C. Bloom,²⁰ S. Chen,²⁰ W. T. Ford,²⁰ J. F. Hirschauer,²⁰ A. Kreisel,²⁰ M. Nagel,²⁰ U. Nauenberg,²⁰ A. Olivas,²⁰ J. G. Smith,²⁰ K. A. Ulmer,²⁰ S. R. Wagner,²⁰ J. Zhang,²⁰ A. M. Gabareen,²¹ A. Soffer,^{21,†} W. H. Toki,²¹ R. J. Wilson,²¹ F. Winklmeier,²¹ D. D. Altenburg,²² E. Feltresi,²² A. Hauke,²² H. Jasper,²² J. Merkel,²² A. Petzold,²² B. Spaan,²² K. Wacker,²² V. Klose,²³ M. J. Kobel,²³ H. M. Lacker,²³ W. F. Mader,²³ R. Nogowski,²³ J. Schubert,²³ K. R. Schubert,²³ R. Schwierz,²³ J. E. Sundermann,²³ A. Volk,²³ D. Bernard,²⁴ G. R. Bonneaud,²⁴ E. Latour,²⁴ V. Lombardo,²⁴ Ch. Thiebaut,²⁴ M. Verderi,²⁴ P. J. Clark,²⁵ W. Gradl,²⁵ F. Muheim,²⁵ S. Playfer,²⁵ A. I. Robertson,²⁵ J. E. Watson,²⁵ Y. Xie,²⁵ M. Andreotti,²⁶ D. Bettoni,²⁶ C. Bozzi,²⁶ R. Calabrese,²⁶ A. Cecchi,²⁶ G. Cibinetto,²⁶ P. Franchini,²⁶ E. Luppi,²⁶ M. Negrini,²⁶ A. Petrella,²⁶ L. Piemontese,²⁶ E. Prencipe,²⁶ V. Santoro,²⁶ F. Anulli,²⁷ R. Baldini-Ferrolì,²⁷ A. Calcaterra,²⁷ R. de Sangro,²⁷ G. Finocchiaro,²⁷ S. Pacetti,²⁷ P. Patteri,²⁷ I. M. Peruzzi,^{27,‡} M. Piccolo,²⁷ M. Rama,²⁷ A. Zallo,²⁷ A. Buzzo,²⁸ R. Contri,²⁸ M. Lo Vetere,²⁸ M. M. Macri,²⁸ M. R. Monge,²⁸ S. Passaggio,²⁸ C. Patrignani,²⁸ E. Robutti,²⁸ A. Santroni,²⁸ S. Tosi,²⁸ K. S. Chaisanguanthum,²⁹ M. Morii,²⁹ J. Wu,²⁹ R. S. Dubitzky,³⁰ J. Marks,³⁰ S. Schenk,³⁰ U. Uwer,³⁰ D. J. Bard,³¹ P. D. Dauncey,³¹ R. L. Flack,³¹ J. A. Nash,³¹ W. Panduro Vazquez,³¹ M. Tibbetts,³¹ P. K. Behera,³² X. Chai,³² M. J. Charles,³² U. Mallik,³² J. Cochran,³³ H. B. Crawley,³³ L. Dong,³³ V. Eyges,³³ W. T. Meyer,³³ S. Prell,³³ E. I. Rosenberg,³³ A. E. Rubin,³³ Y. Y. Gao,³⁴ A. V. Gritsan,³⁴ Z. J. Guo,³⁴ C. K. Lae,³⁴ A. G. Denig,³⁵ M. Fritsch,³⁵ G. Schott,³⁵ N. Arnaud,³⁶ J. Béguilleux,³⁶ A. D'Orazio,³⁶ M. Davier,³⁶ G. Grosdidier,³⁶ A. Höcker,³⁶ V. Lepeltier,³⁶ F. Le Diberder,³⁶ A. M. Lutz,³⁶ S. Pruvot,³⁶ S. Rodier,³⁶ P. Roudeau,³⁶ M. H. Schune,³⁶ J. Serrano,³⁶ V. Sordini,³⁶ A. Stocchi,³⁶ W. F. Wang,³⁶ G. Wormser,³⁶ D. J. Lange,³⁷ D. M. Wright,³⁷ I. Bingham,³⁸ J. P. Burke,³⁸ C. A. Chavez,³⁸ J. R. Fry,³⁸ E. Gabathuler,³⁸ R. Gamet,³⁸ D. E. Hutchcroft,³⁸ D. J. Payne,³⁸ K. C. Schofield,³⁸ C. Touramanis,³⁸ A. J. Bevan,³⁹ K. A. George,³⁹ F. Di Lodovico,³⁹ R. Sacco,³⁹ G. Cowan,⁴⁰ H. U. Flaecher,⁴⁰ D. A. Hopkins,⁴⁰ S. Paramesvaran,⁴⁰ F. Salvatore,⁴⁰ A. C. Wren,⁴⁰ D. N. Brown,⁴¹ C. L. Davis,⁴¹ J. Allison,⁴² D. Bailey,⁴² N. R. Barlow,⁴² R. J. Barlow,⁴² Y. M. Chia,⁴² C. L. Edgar,⁴² G. D. Lafferty,⁴² T. J. West,⁴² J. I. Yi,⁴² J. Anderson,⁴³ C. Chen,⁴³ A. Jawahery,⁴³ D. A. Roberts,⁴³ G. Simi,⁴³ J. M. Tuggle,⁴³ G. Blaylock,⁴⁴ C. Dallapiccola,⁴⁴ S. S. Hertzbach,⁴⁴ X. Li,⁴⁴ T. B. Moore,⁴⁴ E. Salvati,⁴⁴ S. Saremi,⁴⁴ R. Cowan,⁴⁵ D. Dujmic,⁴⁵ P. H. Fisher,⁴⁵ K. Koeneke,⁴⁵ G. Sciolla,⁴⁵ M. Spitznagel,⁴⁵ F. Taylor,⁴⁵ R. K. Yamamoto,⁴⁵ M. Zhao,⁴⁵ Y. Zheng,⁴⁵ S. E. Mclachlin,^{46,*} P. M. Patel,⁴⁶ S. H. Robertson,⁴⁶ A. Lazzaro,⁴⁷ F. Palombo,⁴⁷ J. M. Bauer,⁴⁸ L. Cremaldi,⁴⁸ V. Eschenburg,⁴⁸ R. Godang,⁴⁸ R. Kroeger,⁴⁸ D. A. Sanders,⁴⁸ D. J. Summers,⁴⁸ H. W. Zhao,⁴⁸ S. Brunet,⁴⁹ D. Côté,⁴⁹ M. Simard,⁴⁹ P. Taras,⁴⁹ F. B. Viaud,⁴⁹ H. Nicholson,⁵⁰ G. De Nardo,⁵¹ F. Fabozzi,^{51,§} L. Lista,⁵¹ D. Monorchio,⁵¹ C. Sciacca,⁵¹ M. A. Baak,⁵² G. Raven,⁵² H. L. Snoek,⁵² C. P. Jessop,⁵³ K. J. Knoepfel,⁵³ J. M. LoSecco,⁵³ G. Benelli,⁵⁴ L. A. Corwin,⁵⁴ K. Honscheid,⁵⁴ H. Kagan,⁵⁴ R. Kass,⁵⁴ J. P. Morris,⁵⁴ A. M. Rahimi,⁵⁴ J. J. Regensburger,⁵⁴ S. J. Sekula,⁵⁴ Q. K. Wong,⁵⁴ N. L. Blount,⁵⁵ J. Brau,⁵⁵ R. Frey,⁵⁵ O. Igonkina,⁵⁵ J. A. Kolb,⁵⁵ M. Lu,⁵⁵ R. Rahmat,⁵⁵ N. B. Sinev,⁵⁵ D. Strom,⁵⁵ J. Strube,⁵⁵ E. Torrence,⁵⁵ N. Gagliardi,⁵⁶ A. Gaz,⁵⁶ M. Margoni,⁵⁶ M. Morandin,⁵⁶ A. Pompili,⁵⁶ M. Posocco,⁵⁶ M. Rotondo,⁵⁶ F. Simonetto,⁵⁶ R. Stroili,⁵⁶ C. Voci,⁵⁶ E. Ben-Haim,⁵⁷ H. Briand,⁵⁷ G. Calderini,⁵⁷ J. Chauveau,⁵⁷ P. David,⁵⁷ L. Del Buono,⁵⁷ Ch. de la Vaissière,⁵⁷ O. Hamon,⁵⁷ Ph. Leruste,⁵⁷ J. Malclès,⁵⁷ J. Ocariz,⁵⁷ A. Perez,⁵⁷ J. Prendki,⁵⁷ L. Gladney,⁵⁸ M. Biasini,⁵⁹ R. Covarelli,⁵⁹ E. Manoni,⁵⁹ C. Angelini,⁶⁰ G. Batignani,⁶⁰

S. Bettarini,⁶⁰ M. Carpinelli,⁶⁰ R. Cenci,⁶⁰ A. Cervelli,⁶⁰ F. Forti,⁶⁰ M. A. Giorgi,⁶⁰ A. Lusiani,⁶⁰ G. Marchiori,⁶⁰ M. A. Mazur,⁶⁰ M. Morganti,⁶⁰ N. Neri,⁶⁰ E. Paoloni,⁶⁰ G. Rizzo,⁶⁰ J. J. Walsh,⁶⁰ J. Biesiada,⁶¹ P. Elmer,⁶¹ Y. P. Lau,⁶¹ C. Lu,⁶¹ J. Olsen,⁶¹ A. J. S. Smith,⁶¹ A. V. Telnov,⁶¹ E. Baracchini,⁶² F. Bellini,⁶² G. Cavoto,⁶² D. del Re,⁶² E. Di Marco,⁶² R. Faccini,⁶² F. Ferrarotto,⁶² F. Ferroni,⁶² M. Gaspero,⁶² P. D. Jackson,⁶² L. Li Gioi,⁶² M. A. Mazzoni,⁶² S. Morganti,⁶² G. Piredda,⁶² F. Polci,⁶² F. Renga,⁶² C. Voena,⁶² M. Ebert,⁶³ T. Hartmann,⁶³ H. Schröder,⁶³ R. Waldi,⁶³ T. Adye,⁶⁴ G. Castelli,⁶⁴ B. Franek,⁶⁴ E. O. Olaiya,⁶⁴ W. Roethel,⁶⁴ F. F. Wilson,⁶⁴ S. Emery,⁶⁵ M. Escalier,⁶⁵ A. Gaidot,⁶⁵ S. F. Ganzhur,⁶⁵ G. Hamel de Monchenault,⁶⁵ W. Kozanecki,⁶⁵ G. Vasseur,⁶⁵ Ch. Yèche,⁶⁵ M. Zito,⁶⁵ X. R. Chen,⁶⁶ H. Liu,⁶⁶ W. Park,⁶⁶ M. V. Purohit,⁶⁶ R. M. White,⁶⁶ J. R. Wilson,⁶⁶ M. T. Allen,⁶⁷ D. Aston,⁶⁷ R. Bartoldus,⁶⁷ P. Bechtel,⁶⁷ R. Claus,⁶⁷ J. P. Coleman,⁶⁷ M. R. Convery,⁶⁷ J. C. Dingfelder,⁶⁷ J. Dorfan,⁶⁷ G. P. Dubois-Felsmann,⁶⁷ W. Dunwoodie,⁶⁷ R. C. Field,⁶⁷ T. Glanzman,⁶⁷ S. J. Gowdy,⁶⁷ M. T. Graham,⁶⁷ P. Grenier,⁶⁷ C. Hast,⁶⁷ W. R. Innes,⁶⁷ J. Kaminski,⁶⁷ M. H. Kelsey,⁶⁷ H. Kim,⁶⁷ P. Kim,⁶⁷ M. L. Kocian,⁶⁷ D. W. G. S. Leith,⁶⁷ S. Li,⁶⁷ S. Luitz,⁶⁷ V. Luth,⁶⁷ H. L. Lynch,⁶⁷ D. B. MacFarlane,⁶⁷ H. Marsiske,⁶⁷ R. Messner,⁶⁷ D. R. Muller,⁶⁷ C. P. O'Grady,⁶⁷ I. Ofte,⁶⁷ A. Perazzo,⁶⁷ M. Perl,⁶⁷ T. Pulliam,⁶⁷ B. N. Ratcliff,⁶⁷ A. Roodman,⁶⁷ A. A. Salnikov,⁶⁷ R. H. Schindler,⁶⁷ J. Schwiening,⁶⁷ A. Snyder,⁶⁷ D. Su,⁶⁷ M. K. Sullivan,⁶⁷ K. Suzuki,⁶⁷ S. K. Swain,⁶⁷ J. M. Thompson,⁶⁷ J. Va'vra,⁶⁷ A. P. Wagner,⁶⁷ M. Weaver,⁶⁷ W. J. Wisniewski,⁶⁷ M. Wittgen,⁶⁷ D. H. Wright,⁶⁷ A. K. Yarritu,⁶⁷ K. Yi,⁶⁷ C. C. Young,⁶⁷ V. Ziegler,⁶⁷ P. R. Burchat,⁶⁸ A. J. Edwards,⁶⁸ S. A. Majewski,⁶⁸ T. S. Miyashita,⁶⁸ B. A. Petersen,⁶⁸ L. Wilden,⁶⁸ S. Ahmed,⁶⁹ M. S. Alam,⁶⁹ R. Bula,⁶⁹ J. A. Ernst,⁶⁹ V. Jain,⁶⁹ B. Pan,⁶⁹ M. A. Saeed,⁶⁹ F. R. Wappler,⁶⁹ S. B. Zain,⁶⁹ M. Krishnamurthy,⁷⁰ S. M. Spanier,⁷⁰ R. Eckmann,⁷¹ J. L. Ritchie,⁷¹ A. M. Ruland,⁷¹ C. J. Schilling,⁷¹ R. F. Schwitters,⁷¹ J. M. Izen,⁷² X. C. Lou,⁷² S. Ye,⁷² F. Bianchi,⁷³ F. Gallo,⁷³ D. Gamba,⁷³ M. Pelliccioni,⁷³ M. Bomben,⁷⁴ L. Bosisio,⁷⁴ C. Cartaro,⁷⁴ F. Cossutti,⁷⁴ G. Della Ricca,⁷⁴ L. Lanceri,⁷⁴ L. Vitale,⁷⁴ V. Azzolini,⁷⁵ N. Lopez-March,⁷⁵ F. Martinez-Vidal,⁷⁵ D. A. Milanes,⁷⁵ A. Oyanguren,⁷⁵ J. Albert,⁷⁶ Sw. Banerjee,⁷⁶ B. Bhuyan,⁷⁶ K. Hamano,⁷⁶ R. Kowalewski,⁷⁶ I. M. Nugent,⁷⁶ J. M. Roney,⁷⁶ R. J. Sobie,⁷⁶ P. F. Harrison,⁷⁷ J. Ilic,⁷⁷ T. E. Latham,⁷⁷ G. B. Mohanty,⁷⁷ H. R. Band,⁷⁸ X. Chen,⁷⁸ S. Dasu,⁷⁸ K. T. Flood,⁷⁸ J. J. Hollar,⁷⁸ P. E. Kutter,⁷⁸ Y. Pan,⁷⁸ M. Pierini,⁷⁸ R. Prepost,⁷⁸ S. L. Wu,⁷⁸ and H. Neal⁷⁹

(BABAR Collaboration)

¹Laboratoire de Physique des Particules, IN2P3/CNRS et Université de Savoie, F-74941 Annecy-Le-Vieux, France

²Universitat de Barcelona, Facultat de Física, Departament ECM, E-08028 Barcelona, Spain

³Università di Bari, Dipartimento di Fisica and INFN, I-70126 Bari, Italy

⁴University of Bergen, Institute of Physics, N-5007 Bergen, Norway

⁵Lawrence Berkeley National Laboratory and University of California, Berkeley, California 94720, USA

⁶University of Birmingham, Birmingham, B15 2TT, United Kingdom

⁷Ruhr Universität Bochum, Institut für Experimentalphysik 1, D-44780 Bochum, Germany

⁸University of Bristol, Bristol BS8 1TL, United Kingdom

⁹University of British Columbia, Vancouver, British Columbia, Canada V6T 1Z1

¹⁰Brunel University, Uxbridge, Middlesex UB8 3PH, United Kingdom

¹¹Budker Institute of Nuclear Physics, Novosibirsk 630090, Russia

¹²University of California at Irvine, Irvine, California 92697, USA

¹³University of California at Los Angeles, Los Angeles, California 90024, USA

¹⁴University of California at Riverside, Riverside, California 92521, USA

¹⁵University of California at San Diego, La Jolla, California 92093, USA

¹⁶University of California at Santa Barbara, Santa Barbara, California 93106, USA

¹⁷University of California at Santa Cruz, Institute for Particle Physics, Santa Cruz, California 95064, USA

¹⁸California Institute of Technology, Pasadena, California 91125, USA

¹⁹University of Cincinnati, Cincinnati, Ohio 45221, USA

²⁰University of Colorado, Boulder, Colorado 80309, USA

²¹Colorado State University, Fort Collins, Colorado 80523, USA

²²Universität Dortmund, Institut für Physik, D-44221 Dortmund, Germany

²³Technische Universität Dresden, Institut für Kern- und Teilchenphysik, D-01062 Dresden, Germany

²⁴Laboratoire Leprince-Ringuet, CNRS/IN2P3, Ecole Polytechnique, F-91128 Palaiseau, France

²⁵University of Edinburgh, Edinburgh EH9 3JZ, United Kingdom

²⁶Università di Ferrara, Dipartimento di Fisica and INFN, I-44100 Ferrara, Italy

²⁷Laboratori Nazionali di Frascati dell'INFN, I-00044 Frascati, Italy

²⁸Università di Genova, Dipartimento di Fisica and INFN, I-16146 Genova, Italy

²⁹Harvard University, Cambridge, Massachusetts 02138, USA

³⁰Universität Heidelberg, Physikalisches Institut, Philosophenweg 12, D-69120 Heidelberg, Germany

- ³¹Imperial College London, London, SW7 2AZ, United Kingdom
³²University of Iowa, Iowa City, Iowa 52242, USA
³³Iowa State University, Ames, Iowa 50011-3160, USA
³⁴Johns Hopkins University, Baltimore, Maryland 21218, USA
³⁵Universität Karlsruhe, Institut für Experimentelle Kernphysik, D-76021 Karlsruhe, Germany
³⁶Laboratoire de l'Accélérateur Linéaire, IN2P3/CNRS et Université Paris-Sud 11, Centre Scientifique d'Orsay, B. P. 34, F-91898 ORSAY Cedex, France
³⁷Lawrence Livermore National Laboratory, Livermore, California 94550, USA
³⁸University of Liverpool, Liverpool L69 7ZE, United Kingdom
³⁹Queen Mary, University of London, E1 4NS, United Kingdom
⁴⁰University of London, Royal Holloway and Bedford New College, Egham, Surrey TW20 0EX, United Kingdom
⁴¹University of Louisville, Louisville, Kentucky 40292, USA
⁴²University of Manchester, Manchester M13 9PL, United Kingdom
⁴³University of Maryland, College Park, Maryland 20742, USA
⁴⁴University of Massachusetts, Amherst, Massachusetts 01003, USA
⁴⁵Massachusetts Institute of Technology, Laboratory for Nuclear Science, Cambridge, Massachusetts 02139, USA
⁴⁶McGill University, Montréal, Québec, Canada H3A 2T8
⁴⁷Università di Milano, Dipartimento di Fisica and INFN, I-20133 Milano, Italy
⁴⁸University of Mississippi, University, Mississippi 38677, USA
⁴⁹Université de Montréal, Physique des Particules, Montréal, Québec, Canada H3C 3J7
⁵⁰Mount Holyoke College, South Hadley, Massachusetts 01075, USA
⁵¹Università di Napoli Federico II, Dipartimento di Scienze Fisiche and INFN, I-80126, Napoli, Italy
⁵²NIKHEF, National Institute for Nuclear Physics and High Energy Physics, NL-1009 DB Amsterdam, The Netherlands
⁵³University of Notre Dame, Notre Dame, Indiana 46556, USA
⁵⁴Ohio State University, Columbus, Ohio 43210, USA
⁵⁵University of Oregon, Eugene, Oregon 97403, USA
⁵⁶Università di Padova, Dipartimento di Fisica and INFN, I-35131 Padova, Italy
⁵⁷Laboratoire de Physique Nucléaire et de Hautes Energies, IN2P3/CNRS, Université Pierre et Marie Curie-Paris6, Université Denis Diderot-Paris7, F-75252 Paris, France
⁵⁸University of Pennsylvania, Philadelphia, Pennsylvania 19104, USA
⁵⁹Università di Perugia, Dipartimento di Fisica and INFN, I-06100 Perugia, Italy
⁶⁰Università di Pisa, Dipartimento di Fisica, Scuola Normale Superiore and INFN, I-56127 Pisa, Italy
⁶¹Princeton University, Princeton, New Jersey 08544, USA
⁶²Università di Roma La Sapienza, Dipartimento di Fisica and INFN, I-00185 Roma, Italy
⁶³Universität Rostock, D-18051 Rostock, Germany
⁶⁴Rutherford Appleton Laboratory, Chilton, Didcot, Oxon, OX11 0QX, United Kingdom
⁶⁵DSM/Dapnia, CEA/Saclay, F-91191 Gif-sur-Yvette, France
⁶⁶University of South Carolina, Columbia, South Carolina 29208, USA
⁶⁷Stanford Linear Accelerator Center, Stanford, California 94309, USA
⁶⁸Stanford University, Stanford, California 94305-4060, USA
⁶⁹State University of New York, Albany, New York 12222, USA
⁷⁰University of Tennessee, Knoxville, Tennessee 37996, USA
⁷¹University of Texas at Austin, Austin, Texas 78712, USA
⁷²University of Texas at Dallas, Richardson, Texas 75083, USA
⁷³Università di Torino, Dipartimento di Fisica Sperimentale and INFN, I-10125 Torino, Italy
⁷⁴Università di Trieste, Dipartimento di Fisica and INFN, I-34127 Trieste, Italy
⁷⁵IFIC, Universitat de Valencia-CSIC, E-46071 Valencia, Spain
⁷⁶University of Victoria, Victoria, British Columbia, Canada V8W 3P6
⁷⁷Department of Physics, University of Warwick, Coventry CV4 7AL, United Kingdom
⁷⁸University of Wisconsin, Madison, Wisconsin 53706, USA
⁷⁹Yale University, New Haven, Connecticut 06511, USA

(Received 11 August 2007; published 26 December 2007)

We present an updated measurement of the CP -odd fraction and the time-dependent CP asymmetries in the decay $B^0 \rightarrow D^{*+} D^{*-}$ using $(383 \pm 4) \times 10^6 B\bar{B}$ pairs collected with the BABAR detector. We

*Deceased

†Now at Tel Aviv University, Tel Aviv, 69978, Israel

‡Also with Università di Perugia, Dipartimento di Fisica, Perugia, Italy

§Also with Università della Basilicata, Potenza, Italy

||Also with Universitat de Barcelona, Facultat de Física, Departament ECM, E-08028 Barcelona, Spain

determine the CP -odd fraction to be $0.143 \pm 0.034(\text{stat}) \pm 0.008(\text{syst})$. The time-dependent CP asymmetry parameters are determined to be $C_+ = -0.05 \pm 0.14(\text{stat}) \pm 0.02(\text{syst})$ and $S_+ = -0.72 \pm 0.19(\text{stat}) \pm 0.05(\text{syst})$. The nonzero value of the measured S_+ indicates the evidence of CP violation at the 3.7σ confidence level.

DOI: [10.1103/PhysRevD.76.111102](https://doi.org/10.1103/PhysRevD.76.111102)

PACS numbers: 13.25.Hw, 11.30.Er, 12.15.Hh

In the standard model (SM), CP violation is described by a single complex phase in the Cabibbo-Kobayashi-Maskawa (CKM) quark-mixing matrix, V [1]. Measurements of CP asymmetries by the *BABAR* [2] and Belle [3] collaborations have firmly established this effect in the $b \rightarrow (c\bar{c})s$ charmonium decays [4] and precisely determined the parameter $\sin 2\beta$, where β is $\arg[-V_{cd}V_{cb}^*/V_{td}V_{tb}^*]$. The amplitude of the decay $B^0 \rightarrow D^{*+}D^{*-}$ is dominated by a tree-level, color-allowed $b \rightarrow c\bar{c}d$ transition. Within the framework of the SM, the CP asymmetry of $B^0 \rightarrow D^{*+}D^{*-}$ is equal to $\sin 2\beta$ when the correction due to penguin diagram contributions is neglected. The penguin-induced correction to the CP asymmetry, estimated in models based on the factorization approximation and heavy quark symmetry, is predicted to be about 2% [5], while contributions from non-SM processes may lead to a large correction [6]. Such a deviation in the $\sin 2\beta$ measurement from that of the $B^0 \rightarrow (c\bar{c})K^{(*)0}$ decays would be evidence of physics beyond the SM.

Studies of CP violation in $B^0 \rightarrow D^{(*)\pm}D^{(*)\mp}$ transitions have been carried out by both the *BABAR* and Belle collaborations. Most recently, the Belle collaboration reported evidence of large direct CP violation in $B^0 \rightarrow D^+D^-$ where $C_{D^+D^-} = -0.91 \pm 0.23 \pm 0.06$ [7], in contradiction to the SM expectation. However, a large direct CP violation has not been observed in this channel by *BABAR* [8], nor in previous measurements with $B^0 \rightarrow D^{*+}D^{*-}$ decays that involve the same quark-level weak decay [9,10].

The $B^0 \rightarrow D^{*+}D^{*-}$ decay proceeds through the CP -even S and D waves and through the CP -odd P wave. In this paper, we present an improved measurement of the CP -odd fraction R_\perp based on a time-integrated one-dimensional angular analysis. We also present an improved measurement of the time-dependent CP asymmetry, obtained from a combined analysis of time-dependent flavor-tagged decays and the one-dimensional angular distribution of the decay products.

The data used in this analysis comprise $(383 \pm 4) \times 10^6$ $Y(4S) \rightarrow B\bar{B}$ decays collected with the *BABAR* detector [11] at the PEP-II asymmetric-energy e^+e^- storage rings. We use a Monte Carlo (MC) simulation based on GEANT4 [12] to validate the analysis procedure and to study the relevant backgrounds.

We select $B^0 \rightarrow D^{*+}D^{*-}$ candidates from oppositely charged pairs of D^* mesons. The D^{*+} is reconstructed in

its decays to $D^0\pi^+$ and $D^+\pi^0$. We reconstruct candidates for D^0 and D^+ mesons in the modes $D^0 \rightarrow K^-\pi^+$, $K^-\pi^+\pi^0$, $K^-\pi^+\pi^+\pi^-$, $K_S^0\pi^+\pi^-$ and $D^+ \rightarrow K^-\pi^+\pi^+$. We reject the B^0 candidates for which both D^* mesons decay to $D\pi^0$ because of the smaller branching fraction and larger backgrounds. To suppress the $e^+e^- \rightarrow q\bar{q}$ ($q = u, d, s$, and c) continuum background, we require the ratio of the second and zeroth order Fox-Wolfram moments [13] to be less than 0.6.

For each $B^0 \rightarrow D^{*+}D^{*-}$ candidate, we construct a likelihood function $\mathcal{L}_{\text{mass}}$ from the masses and mass uncertainties of the D and D^* candidates [14]. In this likelihood, the D mass resolution is modeled by a Gaussian function whose variance is determined candidate-by-candidate from the mass uncertainty resulting from a vertex fit of the D meson decay products. The $D^* - D$ mass difference resolution is modeled by the sum of two Gaussian distributions whose parameters are determined from simulated events. The maximum allowed values of $-\ln \mathcal{L}_{\text{mass}}$ and $|\Delta E| \equiv |E_B^* - E_{\text{beam}}|$, the difference between the B^0 candidate energy E_B^* and the beam energy E_{beam} in the $Y(4S)$ frame, are optimized separately for each final state using simulated events to obtain the highest expected signal significance.

We include candidates with an energy-substituted mass, $m_{\text{ES}} \equiv \sqrt{E_{\text{beam}}^2 - p_B^{*2}}$, greater than $5.23 \text{ GeV}/c^2$, where p_B^* is the B^0 candidate momentum in the $Y(4S)$ frame. On average, we have 1.8 B^0 candidates per event in data after all the selection requirements. In cases where more than one candidate is reconstructed in an event, the candidate with the smallest value of $-\ln \mathcal{L}_{\text{mass}}$ is chosen. Studies using MC samples show that this procedure results in the selection of the correct B^0 candidate more than 95% of the time.

The total probability density function (PDF) of the m_{ES} distribution is the sum of the signal and background components. The signal PDF is modeled by a Gaussian function and the combinatorial background is described by a threshold function [15]. Studies based on MC simulation show that there is a small peaking background from $B^+ \rightarrow \bar{D}^{*0}D^{*+}$ in which a \bar{D}^0 originating from a \bar{D}^{*0} decay is combined with a random soft π^- to form a D^{*-} candidate. This background is described by the same PDF as the signal, and its fraction with respect to the signal yield is fixed to $(1.8 \pm 1.8)\%$, as determined in MC simulation. An unbinned maximum likelihood (ML) fit to the m_{ES} distri-

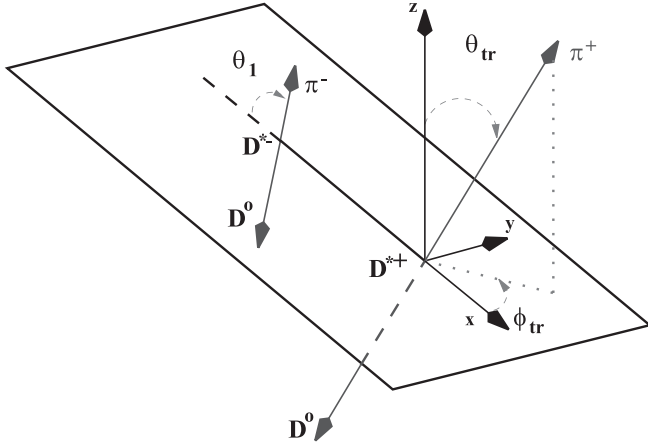


FIG. 1. Depiction of the $B^0 \rightarrow D^{*+} D^{*-}$ decay in the transversity basis. The three transversity angles are defined in the text.

bution yields $617 \pm 33(\text{stat})$ signal events, where the mean and width of the signal Gaussian function and the threshold function shape parameters are allowed to vary in the fit. The signal purity in the region of $m_{\text{ES}} \geq 5.27 \text{ GeV}/c^2$ is approximately 65%.

Following [16], we define three angles depicted in Fig. 1 within the transversity framework: the angle θ_1 between the momentum of the slow pion from the D^{*-} and the direction opposite the D^{*+} flight in the D^{*-} rest frame; the polar angle θ_{tr} and azimuthal angle ϕ_{tr} of the slow pion from the D^{*+} evaluated in the D^{*+} rest frame, where the coordinate system is defined with the z axis normal to the D^{*-} decay plane and the x axis opposite to the D^{*-} momentum.

The time-dependent angular distribution of the decay products is given in Ref. [17]. Taking into account the detector efficiency as a function of the transversity angles and integrating over the decay time and the angles θ_1 and ϕ_{tr} , we obtain a one-dimensional differential decay rate:

$$\frac{1}{\Gamma} \frac{d\Gamma}{d \cos \theta_{\text{tr}}} = \frac{9}{32\pi} \left\{ (1 - R_{\perp}) \sin^2 \theta_{\text{tr}} \times \left[\frac{1 + \alpha}{2} I_0(\cos \theta_{\text{tr}}) + \frac{1 - \alpha}{2} I_{\parallel}(\cos \theta_{\text{tr}}) \right] + 2R_{\perp} \cos^2 \theta_{\text{tr}} \times I_{\perp}(\cos \theta_{\text{tr}}) \right\}, \quad (1)$$

where $R_{\perp} = |A_{\perp}|^2 / (|A_0|^2 + |A_{\parallel}|^2 + |A_{\perp}|^2)$, $\alpha = (|A_0|^2 - |A_{\parallel}|^2) / (|A_0|^2 + |A_{\parallel}|^2)$, A_0 is the amplitude for longitudinally polarized D^* mesons, A_{\parallel} and A_{\perp} are the amplitudes for parallel and perpendicular transversely polarized D^* mesons. The three efficiency moments $I_k(\cos \theta_{\text{tr}})$, where ($k = 0, \parallel, \perp$), are defined as

$$I_k(\cos \theta_{\text{tr}}) = \int d \cos \theta_1 d \phi_{\text{tr}} g_k(\theta_1, \phi_{\text{tr}}) \varepsilon(\theta_1, \theta_{\text{tr}}, \phi_{\text{tr}}), \quad (2)$$

where $g_0 = 4 \cos^2 \theta_1 \cos^2 \phi_{\text{tr}}$, $g_{\parallel} = 2 \sin^2 \theta_1 \sin^2 \phi_{\text{tr}}$, $g_{\perp} = \sin^2 \theta_1$, and ε is the overall detector efficiency. The efficiency moments are parametrized as second-order even polynomials of $\cos \theta_{\text{tr}}$ with parameter values determined from the MC simulation. In fact, the three I_k functions deviate only slightly from a constant, making the decay distribution [Eq. (1)] nearly independent of the amplitude asymmetry α .

The CP -odd fraction R_{\perp} is measured in a simultaneous unbinned ML fit to the $\cos \theta_{\text{tr}}$ and the m_{ES} distributions shown in Fig. 2. The background in the $\cos \theta_{\text{tr}}$ distribution is modeled as an even, second-order polynomial, while the signal PDF is given by Eq. (1). The finite detector resolution of the θ_{tr} measurement is modeled by the sum of three Gaussian functions plus a small tail component that accounts for misreconstructed events, where all the parameters are fixed to the values determined in the MC simulation. The resolution function is convolved with the signal PDF in the maximum likelihood fit. We categorize events into three types: $D^{*+} D^{*-} \rightarrow (D^0 \pi^+, \bar{D}^0 \pi^-)$, $(D^0 \pi^+, D^- \pi^0)$, and $(D^+ \pi^0, \bar{D}^0 \pi^-)$, each with different

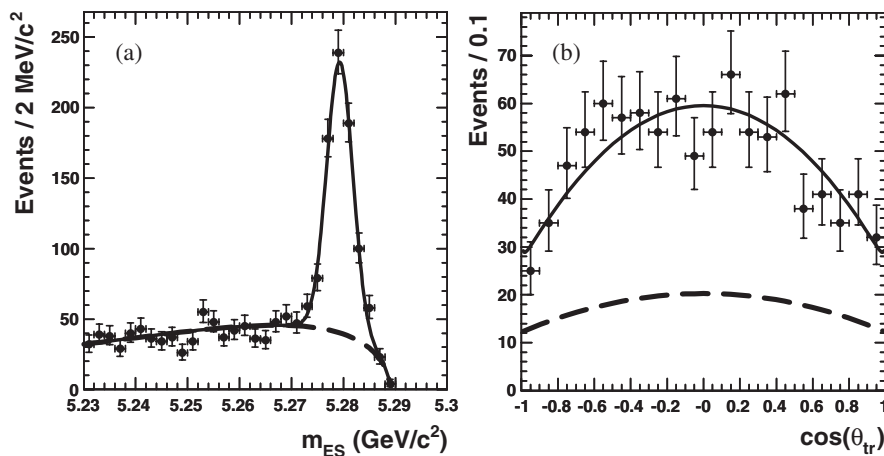


FIG. 2. Measured distribution of m_{ES} (a) and of $\cos \theta_{\text{tr}}$ in the region $m_{\text{ES}} > 5.27 \text{ GeV}/c^2$ (b). The solid line is the projection of the fit result. The dotted line represents the background component.

signal-fraction parameters in the likelihood fit. Their efficiency moments and $\cos\theta_{\text{tr}}$ resolutions are separately determined from the MC simulation. The other parameters, determined in the likelihood fit, are the $\cos\theta_{\text{tr}}$ background-shape parameter, three m_{ES} parameters (width and mean of the signal Gaussian, and the threshold function shape parameter), as well as R_{\perp} .

After fitting to data and taking into account possible systematic uncertainties, we find

$$R_{\perp} = 0.143 \pm 0.034(\text{stat}) \pm 0.008(\text{syst}). \quad (3)$$

Figure 2 shows the projections of the data and the fit result onto m_{ES} and $\cos\theta_{\text{tr}}$.

In the fit described above, the value of α , the asymmetry between the two CP -even amplitudes in the transversity framework, is fixed to zero. We estimate the corresponding systematic uncertainty by varying its value from -1 to $+1$ and find negligible change (0.003) in the fitted value of R_{\perp} . Other systematic uncertainties arise from varying fixed parameters within their errors: the parametrization of the angular resolution (0.006), the determination of the efficiency moments (0.004), and the background parametrization (0.004). The total systematic uncertainty on R_{\perp} is 0.008.

We perform a combined analysis of the $\cos\theta_{\text{tr}}$ distribution and its time dependence to extract the time-dependent CP asymmetry, using the event sample described previously. We use information from the other B meson (B_{tag}) in the event to tag the initial flavor of the fully reconstructed $B^0 \rightarrow D^{*+}D^{*-}$ candidate (B_{rec}). The multivariate flavor tagging algorithm is described in detail elsewhere [18]. We define six mutually exclusive tagging categories in order of expected tag purity from lepton to hadron, which includes kaon and pion tags. The total effective tagging efficiency of this algorithm is $(30.5 \pm 0.4)\%$.

The decay rate f_+ (f_-) for a neutral B meson accompanied by a B^0 (\bar{B}^0) tag is given by

$$f_{\pm}(\Delta t, \cos\theta_{\text{tr}}) \propto e^{-|\Delta t|/\tau_{B^0}} \{G(1 \mp \Delta\omega) \pm (1 - 2\omega) \\ \times [F \sin(\Delta m_d \Delta t) - H \cos(\Delta m_d \Delta t)]\}, \quad (4)$$

where $\Delta t = t_{\text{rec}} - t_{\text{tag}}$ is the difference between the proper decay time of the B_{rec} and B_{tag} mesons, $\tau_{B^0} = (1.530 \pm 0.009)$ ps is the B^0 lifetime, and $\Delta m_d = (0.507 \pm 0.005)$ ps $^{-1}$ is the mass difference between the B^0 - \bar{B}^0 mass eigenstates [19]. The average mistag probability ω describes the effect of incorrect tags, and $\Delta\omega$ is the difference between the mistag rate for B^0 and \bar{B}^0 . The G , F , and H coefficients are defined as:

$$G = (1 - R_{\perp})\sin^2\theta_{\text{tr}} + 2R_{\perp}\cos^2\theta_{\text{tr}}, \\ F = (1 - R_{\perp})S_+\sin^2\theta_{\text{tr}} - 2R_{\perp}S_{\perp}\cos^2\theta_{\text{tr}}, \\ H = (1 - R_{\perp})C_+\sin^2\theta_{\text{tr}} + 2R_{\perp}C_{\perp}\cos^2\theta_{\text{tr}}, \quad (5)$$

where we allow the three transversity amplitudes to have different $\lambda_k = (q/p)(\bar{A}_k/A_k)$ ($k = 0, \parallel, \perp$) [17] due to possibly different penguin-to-tree amplitude ratios, and define the CP asymmetry parameters $C_k = (1 - |\lambda_k|^2)/(1 + |\lambda_k|^2)$, $S_k = 2\text{Im}(\lambda_k)/(1 + |\lambda_k|^2)$. Here, we also define:

$$C_+ = \frac{C_{\parallel}|A_{\parallel}|^2 + C_0|A_0|^2}{|A_{\parallel}|^2 + |A_0|^2}, \quad S_+ = \frac{S_{\parallel}|A_{\parallel}|^2 + S_0|A_0|^2}{|A_{\parallel}|^2 + |A_0|^2}. \quad (6)$$

In the absence of penguin contributions, we expect that $C_0 = C_{\parallel} = C_{\perp} = 0$, and $S_0 = S_{\parallel} = S_{\perp} = -\sin 2\beta$ [5].

In Eq. (4), the small detector efficiency effects are not taken into account and instead are absorbed into the value of R_{\perp} , which is allowed to vary in the final fit. Any bias in the resulting values of C_+ , C_{\perp} , S_+ , and S_{\perp} is below the sensitivity of our MC validation sample and is accounted for in the MC statistics systematic. Hence, a dedicated method to correct for detector efficiency is not required. However, the ‘‘effective’’ value of R_{\perp} obtained in this way is not identical to the value measured from the time-integrated analysis that includes the efficiency correction. This approach incorporates the uncertainty in R_{\perp} directly into the determination of the CP parameters in the ML fit.

The technique used to measure the CP asymmetry is analogous to that used in *BABAR* measurements as described in Ref. [18,20]. We calculate the time interval Δt between the two B decays from the measured separation Δz between the decay vertices of B_{rec} and B_{tag} along the collision (z) axis [20]. The z position of the B_{rec} vertex is determined from the charged daughter tracks. The B_{tag} decay vertex is determined by fitting charged tracks not belonging to the B_{rec} candidate to a common vertex, employing constraints from the beam spot location and the B_{rec} momentum [20]. Only events with a Δt uncertainty less than 2.5 ps and a measured $|\Delta t|$ less than 20 ps are accepted. We perform a simultaneous unbinned ML fit to the $\cos\theta_{\text{tr}}$, Δt , and m_{ES} distributions to extract the CP asymmetry. The signal PDF in θ_{tr} and Δt is given by Eq. (4). The signal mistag probability and the difference between the mistag rate for B^0 and \bar{B}^0 are determined for each tagging category from a large sample of neutral B decays to flavor eigenstates, B_{flav} . In the likelihood fit, the expression in Eq. (4) is convolved with an empirical Δt resolution function determined from the B_{flav} sample. The θ_{tr} resolution is accounted for in the same way as described previously.

Our increased statistics allows for better treatment of the background in this analysis. The background Δt distributions are parametrized by an empirical description that includes components that have zero lifetime, and that have an effective lifetime similar to the signal. The lifetime of the second component and its relative fraction are allowed to vary in the likelihood fit. We also allow the lifetime component to have free effective CP asymmetry parameters, C_{eff} and S_{eff} , for each tagging category to take

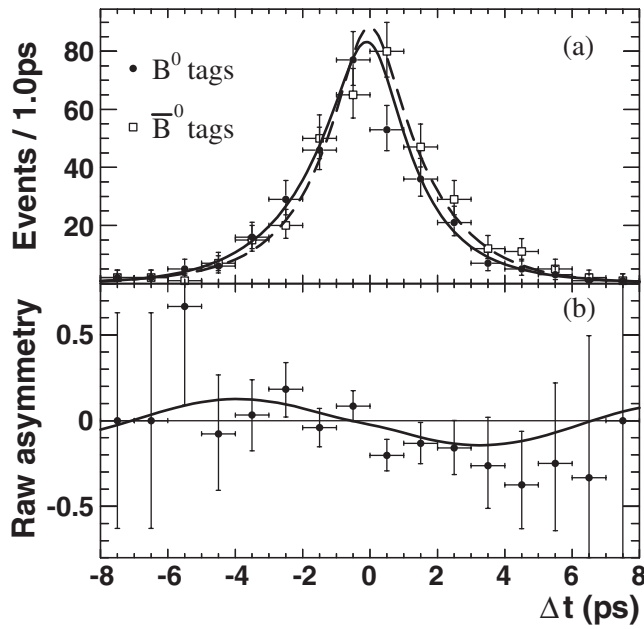


FIG. 3. The distribution in Δt of the yield in the region $m_{ES} > 5.27 \text{ GeV}/c^2$ for $B^0(\bar{B}^0)$ tagged candidates (a) and the raw asymmetry $(N_{B^0} - N_{\bar{B}^0})/(N_{B^0} + N_{\bar{B}^0})$, as functions of Δt (b). In (a), the solid (dashed) curves represent the fit to the data for $B^0(\bar{B}^0)$ tags.

into account a possible difference in mistag rates in the background. The background shape in θ_{tr} is modeled by an even, second-order polynomial in $\cos\theta_{tr}$, as in the time-integrated angular analysis.

From our fit to data we determine

$$\begin{aligned} C_+ &= -0.05 \pm 0.14(\text{stat}) \pm 0.02(\text{syst}), \\ C_\perp &= 0.23 \pm 0.67(\text{stat}) \pm 0.10(\text{syst}), \\ S_+ &= -0.72 \pm 0.19(\text{stat}) \pm 0.05(\text{syst}), \\ S_\perp &= -1.83 \pm 1.04(\text{stat}) \pm 0.23(\text{syst}). \end{aligned} \quad (7)$$

The correlations between C_+ and C_- and between S_+ and S_- are -0.46 and 0.39 , respectively. All other correlations are negligible. Figure 3 shows the Δt distributions and

asymmetry in yield between B^0 and \bar{B}^0 tags, overlaid with the result of the likelihood fit. Because R_\perp is small, we have rather large statistical uncertainties for the measured C_\perp and S_\perp values. We repeat the fit assuming that both CP -even and CP -odd states have the same CP asymmetry, i.e. $C_+ = C_\perp = C$ and $S_+ = S_\perp = S$. We find

$$\begin{aligned} C &= -0.02 \pm 0.11(\text{stat}) \pm 0.02(\text{syst}), \\ S &= -0.66 \pm 0.19(\text{stat}) \pm 0.04(\text{syst}). \end{aligned} \quad (8)$$

In both cases, the effective CP asymmetries in the background are found to be consistent with zero. To further test the consistency of the fitting procedure, the same analysis is applied to the $B^0 \rightarrow D_s^{*+} D^{*-}$ control sample. The result is consistent with no CP violation as expected.

The sources of systematic uncertainty on the CP asymmetries and their estimated magnitudes are summarized in Table I. We vary the yield and CP asymmetries of possible backgrounds that peak under the signal. We also vary fixed parameters in the fit for the assumed parameterization of the Δt resolution function, the possible differences between the B_{flav} and B_{CP} mistag fractions, and knowledge of the event-by-event beam-spot position. We evaluate the uncertainty due to possible interference between the suppressed $b \rightarrow u\bar{c}d$ amplitude and the favored $b \rightarrow c\bar{u}d$ amplitude for some tag side decays [21]. We also include systematic uncertainties incurred from the finite MC sample used to verify the fitting method. All of the systematic uncertainties are much smaller than the statistical uncertainties.

In summary, we have reported measurements of the CP -odd fraction, R_\perp , and time-dependent CP asymmetries for the decay $B^0 \rightarrow D^{*+} D^{*-}$. The measurement is consistent with and supersedes the previous *BABAR* result [9]. The time-dependent asymmetries are found to be consistent with the SM predictions. The nonzero value of the measured S_+ indicates the evidence of CP violation at the 3.7σ confidence level.

We are grateful for the excellent luminosity and machine conditions provided by our PEP-II colleagues, and for the substantial dedicated effort from the computing organiza-

TABLE I. Systematic errors on time-dependent CP asymmetry parameters for the decay $B^0 \rightarrow D^{*+} D^{*-}$.

Source	C_+	S_+	C_\perp	S_\perp	C	S
Peaking backgrounds	0.008	0.028	0.037	0.110	0.003	0.028
Δt resolution parametrization	0.009	0.011	0.018	0.022	0.008	0.010
Mistag fraction differences	0.008	0.024	0.016	0.035	0.008	0.024
Beam-spot position	0.004	0.007	0.019	0.042	0.003	0.005
$\Delta m_d, \tau_B$	0.004	0.006	0.016	0.004	0.001	0.006
Angular resolution	0.009	0.031	0.076	0.116	0.008	0.012
Tag-side interference and others	0.014	0.009	0.017	0.021	0.014	0.009
MC statistics	0.005	0.013	0.031	0.150	0.001	0.013
Total	0.024	0.053	0.098	0.229	0.021	0.044

B. AUBERT *et al.*

PHYSICAL REVIEW D **76**, 111102(R) (2007)

tions that support *BABAR*. The collaborating institutions wish to thank SLAC for its support and kind hospitality. This work is supported by DOE and NSF (USA), NSERC (Canada), CEA and CNRS-IN2P3 (France), BMBF and DFG (Germany), INFN (Italy), FOM (The Netherlands),

NFR (Norway), MIST (Russia), MEC (Spain), and STFC (United Kingdom). Individuals have received support from the Marie Curie EIF (European Union) and the A. P. Sloan Foundation.

-
- [1] N. Cabibbo, Phys. Rev. Lett. **10**, 531 (1963); M. Kobayashi and T. Maskawa, Prog. Theor. Phys. **49**, 652 (1973).
 - [2] B. Aubert *et al.* (*BABAR* Collaboration), Phys. Rev. Lett. **89**, 201802 (2002).
 - [3] K. Abe *et al.* (Belle Collaboration), Phys. Rev. D **66**, 071102 (2002).
 - [4] We imply charge conjugate modes throughout the paper.
 - [5] X. Y. Pham and Z. Z. Xing, Phys. Lett. B **458**, 375 (1999).
 - [6] Y. Grossman and M. P. Worah, Phys. Lett. B **395**, 241 (1997).
 - [7] S. Fratina *et al.* (Belle Collaboration), Phys. Rev. Lett. **98**, 221802 (2007).
 - [8] B. Aubert *et al.* (*BABAR* Collaboration), Phys. Rev. Lett. **99**, 071801 (2007).
 - [9] B. Aubert *et al.* (*BABAR* Collaboration), Phys. Rev. Lett. **95**, 151804 (2005).
 - [10] H. Miyake *et al.* (Belle Collaboration), Phys. Lett. B **618**, 34 (2005).
 - [11] B. Aubert *et al.* (*BABAR* Collaboration), Nucl. Instrum. Methods Phys. Res., Sect. A **479**, 1 (2002).
 - [12] S. Agostinelli *et al.* (GEANT4 Collaboration), Nucl. Instrum. Methods Phys. Res., Sect. A **506**, 250 (2003).
 - [13] G. C. Fox and S. Wolfram, Phys. Rev. Lett. **41**, 1581 (1978).
 - [14] B. Aubert *et al.* (*BABAR* Collaboration), Phys. Rev. D **73**, 112004 (2006).
 - [15] H. Albrecht *et al.* (ARGUS Collaboration), Z. Phys. C **48**, 543 (1990).
 - [16] I. Dunietz, H. R. Quinn, A. Snyder, W. Toki, and H. J. Lipkin, Phys. Rev. D **43**, 2193 (1991).
 - [17] The *BABAR* Collaboration Physics Book, edited by P. F. Harrison and H. R. Quinn, SLAC-R504 (1998), pp. 213–220.
 - [18] B. Aubert *et al.* (*BABAR* Collaboration), Phys. Rev. Lett. **94**, 161803 (2005).
 - [19] W. M. Yao *et al.* (Particle Data Group), J. Phys. G **33**, 1 (2006).
 - [20] B. Aubert *et al.* (*BABAR* Collaboration), Phys. Rev. D **66**, 032003 (2002).
 - [21] O. Long, M. Baak, R. N. Cahn, and D. Kirkby, Phys. Rev. D **68**, 034010 (2003).